THE AMERICAN MINERALOGIST
JOURNAL OF THE MINERALOGICAL SOCIETY OF AMERICA

Vol. 48 JANUARY-FEBRUARY, 1963 Nos. 1 and 2

THE CRYSTAL STRUCTURE OF CARMINITE

J. J. FINNEY,[1] *Department of Geology, University of Wisconsin, Madison, Wisconsin.*

ABSTRACT

Carminite, $8[PbFe_2(AsO_4)_2(OH)_2]$, is orthorhombic *Cccm* or *Ccc*2, $a = 16.595$, $b = 7.580$, $c = 12.295$, all ±.005 Å. The structure was determined by means of Patterson, Fourier and difference maps and refined by least squares. The final R-factor is 10.8%. Both centric and noncentric cycles were attempted, but the noncentric cycles converged essentially to the centric structure. The structure consists of octahedra of oxygen and hydroxyl about iron connected to each other by an edge at the mirror plane and by a corner at a two fold axis. The octahedra extend unbroken parallel to the Z-direction in projection on (010) and are connected together in the X-direction by arsenate tetrahedra. Coordination about the lead atoms is eight fold. The structure of carminite is very similar to that of brackebuschite.

INTRODUCTION

Since the original determination of the space group and unit cell of carminite, $PbFe_2(AsO_4)_2(OH)_2$, by Rosenzweig and Finney (1959), similarities between carminite and other minerals have been observed. Recently Strunz (1960) has shown that carminite and palermoite, $SrAl_2(PO_4)_2(OH)_2$, are isotypic and further that these two minerals bear some relation to the minerals of the descloizite series such as conichalcite, $CaCu(AsO_4)(OH)$, and duftite, $PbCu(AsO_4)(OH)$. Donaldson and Barnes (1954) have determined the structure of pyrobelonite, $PbMn(VO_4)(OH)$, another member of this family having the same general formula. The cell dimensions of palermoite ($a = 7.31$, $b = 15.79$, $c = 11.53$ Å) are similar to those of carminite ($a = 16.595$, $b = 7.580$, $c = 12.295$ Å), and the space group is the same (Mrose, 1953).

A close relationship appears to exist with brackebuschite, $Pb_2(Mn,Fe)(VO_4).H_2O$ (Donaldson and Barnes, 1955). The cell dimensions of brackebuschite are $a = 7.681$, $b = 6.155$, $c = 16.524$ Å, $\beta = 93°45'$ for space group $B\ 2_1/m$. If the b-axis of brackebuschite is doubled the dimensions are almost identical with those of carminite. However brackebuschite is monoclinic and carminite is orthorhombic and the Pb:Fe ratio is 1:2 for carminite and the Pb:(Mn,Fe) ratio is 2:1 for brackebuschite. Evidently

---

[1] Present address: Department of Geological Engineering, Colorado School of Mines, Golden, Colorado.

the change of the Pb:(Mn,Fe) ratio in favor of the small cation is not sufficient to cause distortion of the structure beyond an adjustment to orthorhombic symmetry.

Donaldson and Barnes have concluded that though some relationship exists between brackebuschite and the descloizite family, brackebuschite cannot be considered a member of that group of minerals.

Throughout this investigation, the formula used for carminite is that determined by Foshag (1937) and confirmed by LeMesurier (1939).

EXPERIMENTAL WORK

The sample of carminite, from Mapimi, Mexico, used for the original unit cell and space group determination was used also throughout this investigation. The experimental work was carried out with a crystal having the dimensions .043×.300×.048 mm corresponding to the crystallographic axes *a*, *b* and *c* respectively. Data were collected by means of multiple film pack Weissenberg photographs of the *h*0*l*, *h*1*l*, *h*2*l*, *h*3*l* and 0*kl* reciprocal levels. Before collection of the 0*kl* data the crystal was cut approximately in the shape of a cube. All intensities were estimated by comparison of known intensities with the reflections on the Weissenberg photographs and corrected for the Lorentz and polarization factors. The large linear absorption coefficient of 381/cm for molybdenum radiation necessitated application of absorption corrections. Transmission factors for cylindrical crystals were used for the *h*0*l*, *h*1*l*, *h*2*l* and *h*3*l* reflections and transmission factors for spherical crystals were applied to the 0*kl* reflections.

The cell dimensions were redetermined by the θ- method of Weisz, Cochran and Cole (1948) as: $a=16.595$, $b=7.580$, $c=12.295$ all $\pm .005$ Å. The calculated density is 5.46. No measured density was obtained from this sample but LeMesurier (1939) observed a specific gravity of 5.22. The cell formula is $Pb_8Fe_{16}(AsO_4)_{16}(OH)_{16}$.

Only those reflections appear which obey the following restrictions:

hkl	$h+k=2n$	
$0kl$	$(k=2n)$	$l=2n$
$h0l$	$(h=2n)$	$l=2n$

The only two space groups compatible with these restrictions are *Cccm* and *Ccc*2 confirming the original determination. Foshag observed the morphology of carminite to be holohedral and on this basis space group *Cccm* was chosen for the initial structure determination. The equivalent positions for *Cccm* are listed in Table 1.

STRUCTURE DETERMINATION

An examination of the *h*0*l* intensities showed the following nonsystematic distribution, where $h=2n$ and $l=2n$ because of space group re-

TABLE 1. EQUIVALENT POSITIONS FOR SPACE GROUP *Cccm*

	$(+\frac{1}{2}, \frac{1}{2}, 0)$
16 (*m*)	$x, y, z; \bar{x}, \bar{y}, \bar{z}; \bar{x}, y, \frac{1}{2}-z; x, \bar{y}, \frac{1}{2}-z; \bar{x}, \bar{y}, z; x, y, \bar{z}; x, \bar{y}, \frac{1}{2}+z; \bar{x}, y, \frac{1}{2}+z$
8 (*l*)	$x, y, 0; \bar{x}, \bar{y}, 0; \bar{x}, y, \frac{1}{2}; \bar{x}, \bar{y}, \frac{1}{2}$
8 (*k*)	$\frac{1}{4}, \frac{1}{4}, z; \frac{1}{4}, \frac{1}{4}, \bar{z}; \frac{1}{4}, \frac{3}{4}, \frac{1}{2}+z; \frac{1}{4}, \frac{3}{4}, \frac{1}{2}-z$
8 (*j*)	$0, \frac{1}{2}, z; 0, \frac{1}{2}, \bar{z}; 0, \frac{1}{2}, \frac{1}{2}+z; 0, \frac{1}{2}, \frac{1}{2}-z$
8 (*i*)	$0, 0, z; 0, 0, \bar{z}; 0, 0, \frac{1}{2}+z; 0, 0, \frac{1}{2}-z$
8 (*h*)	$0, y, \frac{1}{4}; 0, \bar{y}, \frac{1}{4}; 0, y, \frac{3}{4}; 0, \bar{y}, \frac{3}{4}$
8 (*g*)	$x, 0, \frac{1}{4}; \bar{x}, 0, \frac{1}{4}; x, 0, \frac{3}{4}; \bar{x}, 0, \frac{3}{4}$
4 (*f*)	$\frac{1}{4}, \frac{3}{4}, 0; \frac{1}{4}, \frac{1}{4}, \frac{1}{2}$
4 (*e*)	$\frac{1}{4}, \frac{1}{4}, 0; \frac{1}{4}, \frac{3}{4}, \frac{1}{2}$
4 (*d*)	$0, \frac{1}{2}, 0; 0, \frac{1}{2}, \frac{1}{2}$
4 (*c*)	$0, 0, 0; 0, 0, \frac{1}{2}$
4 (*b*)	$0, \frac{1}{2}, \frac{1}{4}; 0, \frac{1}{2}, \frac{3}{4}$
4 (*a*)	$0, 0, \frac{3}{4}; 0, 0, \frac{1}{4}$

quirements. Reflections having $h+l=4n$ were generally strong and those having $h+l=2n$ were generally weak.

Because the lead atoms are the greatest contributor to the structure amplitudes and thus probably determine the majority of phases, these atoms were thought to be located at $x=\frac{1}{4}$, $z=\frac{1}{4}$. However, if the lead atoms occupied an eight fold position such as (*g*) $x,0,\frac{1}{4}$ or (*k*) $\frac{1}{4},\frac{1}{4},z$ reflections in which $h+l=2n$ would appear strong whereas they actually appear as weak reflections. If, instead of an eight fold position set, the lead atoms are placed in two four fold positions such as (*a*) $0,0,\frac{1}{4}$ and (*f*) $\frac{1}{4},\frac{3}{4},0$ general agreement is found between observed and calculated structure amplitudes.

An *h*0*l* Patterson projection was calculated and the resulting map is reproduced in Figure 1A. The peak at $\frac{1}{4},\frac{1}{4}$ represents the lead-lead vector and is produced by a combination of one set (*a*) or (*b*) with another set (*e*) or (*f*). The remaining large peaks can then be explained as lead-arsenic and lead-iron vectors. These are appropriately designated in Fig. 1A. The lead atoms were placed arbitrarily in position set (*a*) and (*f*). With this arrangement the arsenic atoms are situated in (*g*) $x,0,\frac{1}{4}$ where $x=.21$ and (*l*) x,y,0 where $x=.04$. The sixteen iron atoms were placed in (*m*) with the x and z parameters some multiple of $\frac{1}{8}$.

Three dimensional Fourier sections were calculated in the Y-direction using the contributions of the lead atoms only and the resulting maps confirmed the above relationships. The iron parameters were fixed as $x=.38$, $y=.12$ and $z=.135$. In addition, the y parameter for As_2 was fixed as $y=.75$. Difference maps in the Y-direction were calculated. For these maps the contributions of all metal atoms were subtracted and the positions of all oxygen atoms and hydroxyls were determined. The final Fourier projection on (010) is shown in Fig. 1B.

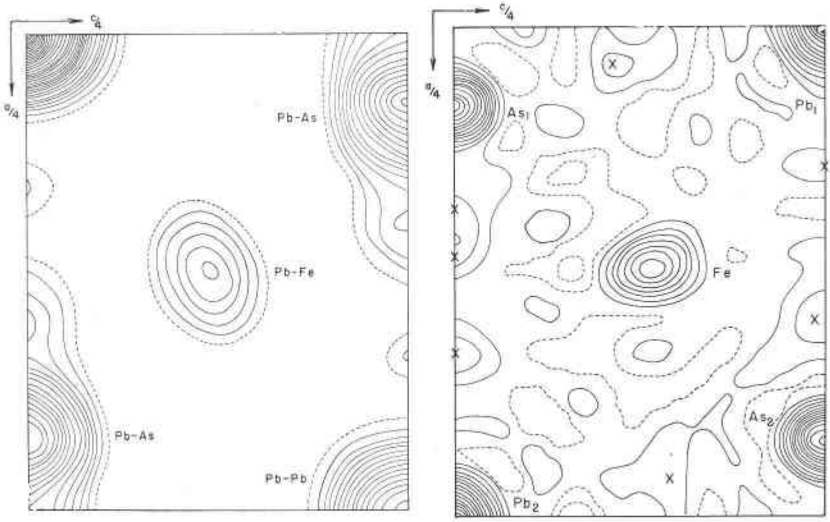

FIG. 1A. (left) Patterson map of carminite projected on (010). Contours are at equal but arbitrary intervals except the origin and Pb-Pb peaks which are twice the contour interval of other peaks. B. (right) Final Fourier map of carminite projected on (010). Contour interval is 10 e/Å^2 except for the peaks representing lead atoms which are 20 e/Å^2. Zero and negative contours are dashed. X indicates the location of oxygen and hydroxyl.

For the initial structure determination the temperature factors $B=1.0$ for lead and $B=.50$ for arsenic and iron were applied to the scattering factors. During all stages of the structure determination and refinement the scattering factors for lead were taken from James and Brindley (1931), for arsenic and oxygen were those determined by Berghuis *et al.* (1955) and for iron the values obtained by Wood and Pratt (1957) were used. Hydroxyl was assumed to have the scattering power of oxygen. All curves were modified for the ionic state. In addition, a real dispersion correction of -4.0 electrons was applied to the scattering factor for lead.

REFINEMENT OF THE STRUCTURE

Refinement of the structure of carminite was effected by use of the method of least squares. The parameters obtained from the Patterson, Fourier and difference maps were used as starting parameters for this refinement. Twenty-two positional parameters, twelve isotropic temperature factors and five scale factors were allowed to vary and the entire 39×39 matrix was computed. All reflections were weighted equally except nonobserved reflections which were weighted zero. Table 2 is a list of the R-factors resulting from the first and final cycles for each reciprocal level.

The standard deviations of the positional parameters were calculated from the formula:

$$\sigma(\xi) = \left(\frac{\sum (\Delta F)^2}{(m - s)} \cdot D_{ii} \right)^{1/2}$$

where m is the number of observations, s is the number of variables and D_{ii} is the diagonal term of the inverse matrix. The final positional parameters and temperature factors together with the standard deviations are listed in Table 3. Large fluctuations of some thermal parameters were observed and the generally large values of the standard deviations of the temperature factors make the thermal parameters unreliable.

TABLE 2. R-FACTORS FROM FIRST AND FINAL CYCLES OF REFINEMENT FOR EACH RECIPROCAL LEVEL

Level	First cycle	Final cycle	Reflections	
h0l	.214	.097		73
h1l	.205	.112		130
h2l	.223	.098		78
h3l	.289	.141		102
0kl	.266	.070		20
Overall	.239	.108	Total observed	403
			Nonobserved	210
			Total	613

Because of the eccentricities of the thermal parameters and their standard deviations, the correlation matrix was calculated for the last cycle. Of the 741 nondiagonal terms of the half-matrix in the correlation matrix, 98 coefficients are larger than .100 and 13 are larger than .300 though none is larger than .520. Thus interactions of thermal parameters are not the primary cause of the large standard deviations and erratic behavior of some temperature factors. Rather they are partially caused by the dominant role of the heavy atoms in the structure and perhaps also by the actual location of As_1, O_2, O_3 and OH_1 off of the mirror plane. This possibility is discussed in a later section.

DISCUSSION OF THE STRUCTURE

Schematic diagrams of the structure of carminite projected on (010) and (100) are shown in Figs. 2 and 3. The arrangement of the oxygen atoms around arsenic atoms is tetrahedral. Within the As_1 tetrahedron the six O–O distances range from 2.77 to 2.92 Å, with a mean distance of 2.84 Å. The 0–0 distances of the As_2 tetrahedron range from 2.59 to 2.72 Å

TABLE 3. FINAL POSITIONAL PARAMETERS, TEMPERATURE FACTORS AND STANDARD DEVIATIONS OF POSITIONAL PARAMETERS FOR CARMINITE

		Parameter	σ			Parameter	σ
$\mathrm{Pb_1}$	x	.000	.000	$\mathrm{O_2}$	x	.0949	.0031
	y	.000	.000		y	.5317	.0120
	z	.250	.000		z	.000	.000
	B	.71	.09		B	2.24	1.01
$\mathrm{Pb_2}$	x	.250	.000	$\mathrm{O_3}$	x	.1136	.0024
	y	.750	.000		y	−.1055	.0111
	z	.000	.000		z	.000	.000
	B	.36	.08		B	—[1]	.60
$\mathrm{As_1}$	x	.0427	.0006	$\mathrm{O_4}$	x	.1525	.0023
	y	.7403	.0029		y	.1741	.0104
	z	.000	.000		z	.2411	.0035
	B	1.68	.21		B	.79	.69
$\mathrm{As_2}$	x	.2111	.0005	$\mathrm{O_5}$	x	.2721	.0022
	y	.000	.000		y	−.0129	.0086
	z	.250	.000		z	.1450	.0030
	B	.70	.15		B	.58	.56
Fe	x	.3778	.0005	$\mathrm{OH_1}$	x	.1656	.0023
	y	.1309	.0021		y	.2589	.0115
	z	.1360	.0006		z	.000	.000
	B	.40	.11		B	—[1]	.55
$\mathrm{O_1}$	x	.0182	.0026	$\mathrm{OH_2}$	x	.4303	.0031
	y	.2404	.0098		y	.000	.000
	z	.1153	.0031		z	.250	.000
	B	.92	.66		B	.90	.97

[1] Thermal parameter tends negative.

with a mean of 2.68 Å. The mean As–O distances are 1.74 Å for the $\mathrm{As_1}$ tetrahedron and 1.64 Å for the $\mathrm{As_2}$ tetrahedron. However because the standard error of the As–O bond length is greater than .10 Å this difference is not significant.

The sixteen iron atoms are located in one sixteen fold position set. They have six nearest neighbors forming an almost regular octahedron at a mean distance from the iron atom of 2.02 Å. Of the six, four are oxygen atoms and two are hydroxyl groups. $\mathrm{O_1}$, $\mathrm{O_2}$, $\mathrm{O_4}$ and $\mathrm{O_5}$ are the oxygen atoms and $\mathrm{OH_1}$ and $\mathrm{OH_2}$ are the hydroxyls. Only $\mathrm{O_3}$ is not bonded to iron. Its distance to the iron atoms of 3.97 Å is significantly larger than the mean of 2.02 Å.

Coordination about the two crystallographically distinct lead atoms is eight fold. The eight neighbors about Pb_1 are made up of four each of O_1 and O_4 while the coordination about Pb_2 is composed of two each of O_3 and O_2 and four of O_5. The mean Pb_1–O distance is 2.67 Å and the mean Pb_2-O distance is 2.69 Å. Table 4 lists all bond lengths and angles and the standard deviations of the bond lengths.

The structure of carminite consists of networks of linked octahedra of oxygen and hydroxyl about iron extending parallel to the *c*-axis. The individual octahedra are joined together on an edge at the mirror plane at $z=0,\frac{1}{2}$ and at a vertex at the two fold rotation axis at $y=0,\frac{1}{2}$ and $z=\frac{1}{4},\frac{3}{4}$. The networks are in turn linked to arsenate tetrahedra. All four vertices of the As_2 tetrahedron are joined also to the vertices of the Fe-O(OH) octahedra, but only three of the vertices of the As_1 tetrahedron are so joined. O_3 is not bonded to an iron atom but only to lead and arsenic. The arsenate groups appear to sit atop one another if the structure is viewed as in Fig. 2. However, as seen in Fig. 3 these are not in contact. The O_1-O_1 distance of the two overlying As_1 tetrahedra is 3.37 Å and the O_5-O_5 distance of the two overlying As_2 tetrahedra is 3.57 Å.

Because the Fe-O(OH) octahedra share an edge on one side and a vertex on the other it was thought that the structure actually belongs in space group *Ccc*2. In the event that carminite is noncentric neither O_2 nor O_3 lie on a mirror plane and instead of only O_2, both O_2 and O_3 would be bonded to Fe. The environment about the two crystallographically distinct arsenic atoms would thus be similar in all respects. Some evidence for this arrangement appears in the results of the least squares refinement. As stated previously the temperature factors of As_1, O_2, O_3 and OH_1 behaved erratically during the course of the refinement, but the fact that these eccentricities are noticed only in the atoms lying on the mirror plane makes the existence of the mirror somewhat suspect.

In order to ascertain whether *Ccc*2 is the true space group or not, a noncentric model of carminite was proposed and a least squares refinement was attempted. Thermal parameter interactions became extreme and it was found necessary to hold temperature factors constant at an arbitrary value. The R-factor decreased to 13% and within the limits of error the structure refined to the original model. It was also found that the systematic absences characteristic of space group *Cccm* and *Ccc*2 could be reproduced accidently by use of a noncentric model in space groups *C*222$_1$ and *C*222. Agreement of observed and calculated structure factors for the *h*0*l*, 0*kl* and *hk*0 reflections was excellent but no agreement was found in the three dimensional data. No evidence contrary to the existence of the mirror plane was observed in the Fourier and difference maps. Still, on the basis of uniformity of environment it is thought that the structure is slightly noncentric.

TABLE 4. INTERATOMIC DISTANCES, BOND ANGLES AND STANDARD DEVIATIONS OF DISTANCES FOR CARMINITE

		Bond length	σ			Bond length	σ
As$_1$-O$_1$	(2)	1.75 Å	.10	As$_2$-O$_4$	(2)	1.64 Å	.10
-O$_2$		1.80	.13	-O$_5$	(2)	1.64	.09
-O$_3$		1.66	.11			——	
		——		Mean		1.64	
Mean		1.74					
O$_1$-O$_1$		2.84	.13	O$_4$-O$_4$		2.65	.14
O$_1$-O$_2$	(2)	2.92	.16	O$_4$-O$_5$	(2)	2.71	.13
O$_1$-O$_3$	(2)	2.80	.15	O$_4$-O$_5$	(2)	2.72	.13
O$_2$-O$_3$		2.77	.17	O$_5$-O$_5$		2.59	.12
		——				——	
Mean		2.84		Mean		2.68	
Fe-O$_1$		2.00	.10	O$_1$-O$_2$		2.92	.16
-O$_2$		2.13	.13	O$_1$-O$_4$		2.76	.14
-O$_4$		2.03	.09	O$_1$-OH$_1$		2.83	.15
-O$_5$		2.07	.09	O$_1$-OH$_2$		2.73	.13
-OH$_1$		2.00	.12	O$_2$-OH$_1$		2.38	.17
-OH$_2$		1.90	.09	O$_2$-OH$_2$		3.10	.16
		——					
Mean		2.02		O$_2$-O$_5$		2.84	.15
				O$_4$-OH$_1$		3.04	.15
				O$_4$-OH$_2$		2.80	.13
				O$_4$-O$_5$		3.03	.13
				O$_5$-OH$_1$		2.82	.14
				O$_5$-OH$_2$		2.87	.12
						——	
				Mean		2.85	
Pb$_1$-O$_1$	(4)	2.48 Å	.09	Pb$_1$-Pb$_1$		$>$4.00	
-O$_4$	(4)	2.86	.10	-Pb$_2$		$>$4.00	
Pb$_2$-O$_2$	(2)	3.06	.13	-As$_1$		3.72	.03
-O$_3$	(2)	2.51	.11	-As$_2$		3.50	.01
-O$_5$	(4)	2.56	.08	-Fe		3.73	.02
Pb$_2$-Pb$_2$		$>$4.00		As$_1$-As$_1$		3.91	.04
-As$_1$		3.44	.03	-As$_2$		$>$4.00	
-As$_2$		3.67	.01	-Fe		3.11	.04
-Fe		3.95	.02	-Fe		3.53	.04
As$_2$-As$_2$		$>$4.00		Fe-Fe		3.44	.03
-Fe		3.26	.02	-Fe		3.44	.03
-Fe		3.56	.02	[1]OH$_2$-OH$_2$		2.44	.13
OH$_1$-OH$_1$		2.80	.16				

[1] Calculated using $x_{OH_2} = .4265$.

TABLE 4—(*Continued*)

	Angle		Angle		Angle
O_1-As_1-O_1	108.5°	O_1-Fe-O_2	89.9°	O_2-Fe-OH_2	100.8°
O_1-As_1-O_2	110.5°	O_1-Fe-O_4	86.5°	O_4-Fe-O_5	98.0°
O_1-As_1-O_3	110.6°	O_1-Fe-OH_1	90.0°	O_4-Fe-OH_1	98.0°
O_1-As_1-O_2	110.6°	O_1-Fe-OH_2	88.9°	O_4-Fe-OH_2	90.9°
O_1-As_1-O_3	110.5°	O_2-Fe-O_5	85.2°	O_5-Fe-OH_1	87.7°
O_2-As_1-O_3	106.1°	O_2-Fe-OH_1	70.2°	O_5-Fe-OH_2	92.6°
Mean	109.5°	Mean	89.9°		
O_4-As_2-O_4	107.4°	O_1-Fe-O_5	175.1°		
O_4-As_2-O_5 (2)	111.6°	O_2-Fe-O_4	167.7°		
O_4-As_2-O_5 (2)	111.1°	OH_1-Fe-OH_2	171.0°		
O_5-As_2-O_5	103.9°				
		Mean	171.2°		
Mean	109.5°				

SIMILARITIES TO BRACKEBUSCHITE

Figure 4 is a projection of the structure of brackebuschite on (100) with the *b*-axis doubled and the origin shifted for easier comparison of the two structures. Brackebuschite contains two crystallographically different lead atoms which are designated Pb_{1b} and Pb_{2b} in Fig. 4. Carminite, on the other hand, can be thought of as having only the site equivalent to Pb_{1b} occupied, though in space group *Cccm* these are two four fold positions. The manganese sites are designated, in brackebuschite, as Mn_{1b} and Mn_{2b}, but only Mn_{1b} is occupied. The vacant positions are marked by X_{Mn2b} in Fig. 4. In carminite, both sites are occupied by iron atoms though symmetry requires a different distribution of *y* parameters (Fig. 2).

In their determination of the structure of brackebuschite, Donaldson and Barnes (1955) tentatively located water molecules above and below the plane of the four oxygen atoms around Mn_{1b}. This position is marked X_{OH} in Fig. 4. The structure of carminite shows that hydroxyl is located in this position as well as in the position occupied by Pb_{2b} in brackebuschite. This produces six fold coordination about the iron atoms in carminite and would be equivalent to six fold coordination about both Mn_{1b} and Mn_{2b} in brackebuschite if Pb_{2b} is considered as OH. Radical distortion has not taken place in carminite because the site formerly occupied by Pb_{2b} in brackebuschite is now occupied by OH, which is approximately the same size as Pb, and the existing octahedral site Mn_{2b} though now filled has not changed size or environment. The bond lengths between

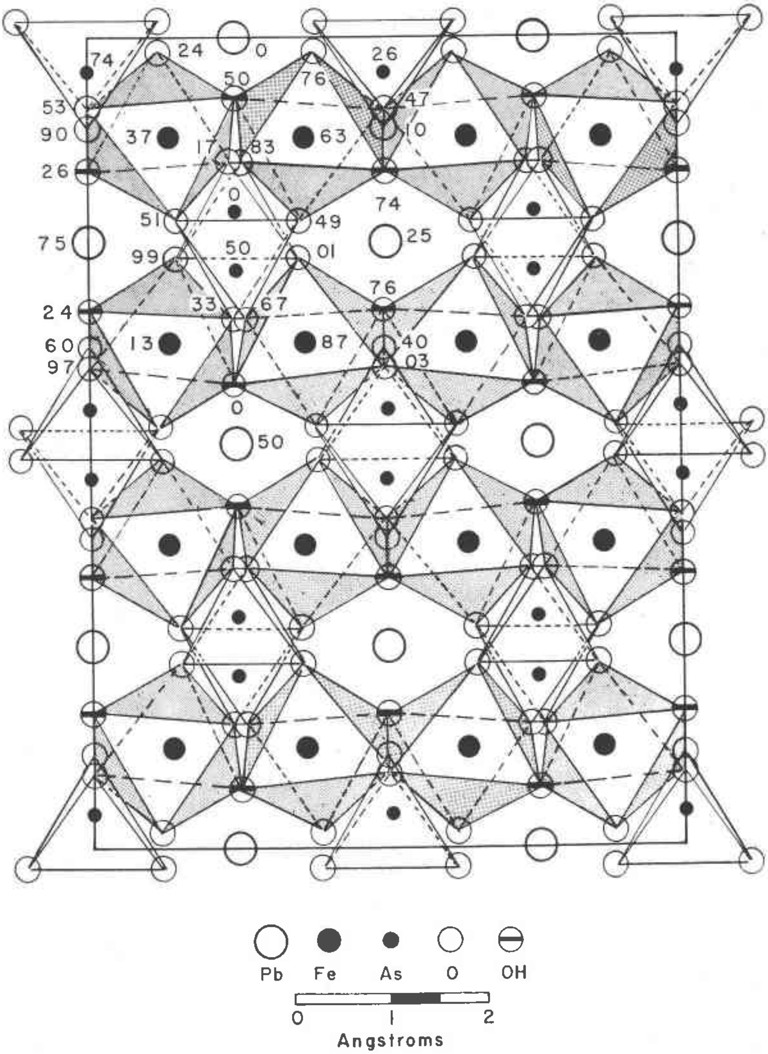

FIG. 2. The structure of carminite projected on (010). The *a*-axis is vertical.

Pb_{2b} and its nearest oxygen neighbors in brackebuschite are 2.58, 2.76, 3.02, 2.64 and 2.83 Å and those for the equivalent position OH_1 in carminite are 2.38, 2.89, 3.24, 2.82 and 2.83 Å.

An intermediate structure type may exist in which a small cation is added to the vacant Mn_{2b} site of brackebuschite with a corresponding removal of the large cation from the Pb_{2b} position to balance charges, with or without changes in the water content.

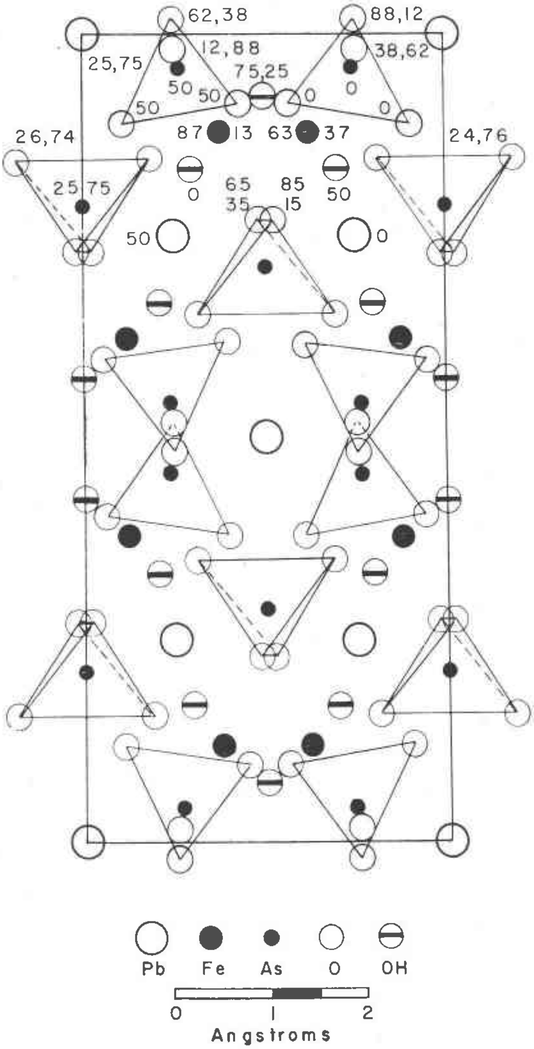

FIG. 3. The structure of carminite projected on (001). The *a*-axis is vertical.

A table listing observed and calculated structure factors for carminite has been deposited as Document No. 7428 with the American Documentation Institute, Auxiliary Publications Project, Photoduplication Service, Library of Congress, Washington 25, D. C. Copies may be secured by citing the document number, and remitting $1.25 for photoprints or $1.25 for 35 mm. microfilm. Advance payment is required.

ACKNOWLEDGMENTS

The author is indebted to Dr. A. Rosenzweig of the University of New

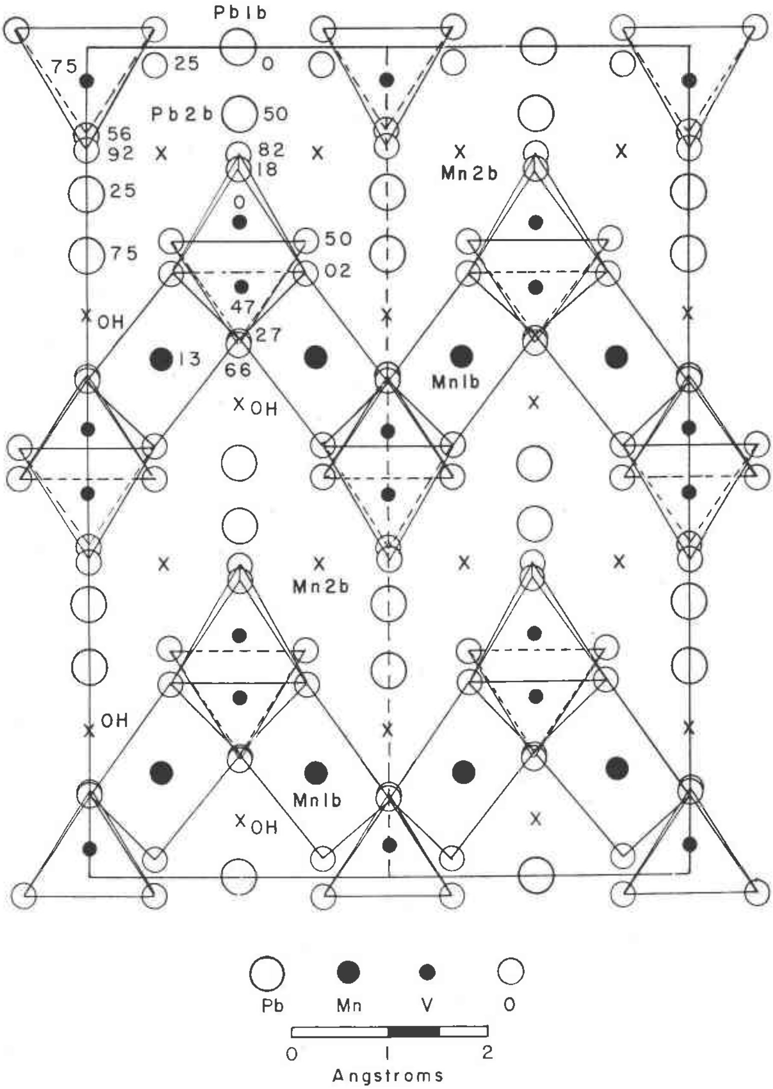

FIG. 4. The structure of brackebuschite projected on (100). $c \sin \beta$ is vertical and the b-axis is doubled.

Mexico who supplied the sample of carminite and gave permission to continue the original work, to Dr. S. W. Bailey of the University of Wisconsin for his advice during the course of the investigation, to D. T. Cromer and to A. C. Larson of the Los Alamos Scientific Laboratory, Los Alamos, New Mexico for their aid in the computation of Fourier and difference syntheses and portions of the least squares refinement. Computer time was graciously supplied by that Laboratory. The Numerical Analysis Laboratory at the University of Wisconsin aided in preparation of programs, data processing and final refinement of the structure. This investigation has been supported by a grant from the National Science Foundation.

REFERENCES

BERGHUIS, J., I. M. HAANAPPEL, M. POTTERS, B. O. LOOPSTRA, C. H. MACGILLAVRY AND A. L. VEENENDAAL (1955) New calculations of atomic scattering factors. *Acta Cryst.* **8,** 478–483.

DONALDSON, D. M. AND W. H. BARNES (1955) The structure of the descloizite and adelite groups, III brackebuschite. *Am. Mineral.* **40,** 597–613.

FOSHAG, W. F. (1937) Carminite and associated minerals from Mapimi, Mexico. *Am. Mineral.* **22,** 479–484.

JAMES, R. W. AND G. W. BRINDLEY (1931) Some numerical calculations of atomic scattering factors. *Phil. Mag.* (7), **12,** 81–112.

LEMESURIER, C. R. (1939) Carminite and budkinite from the Ashburton District. *Jour. Roy. Soc. Western Australia,* **25,** 237.

MROSE, M. E. (1953), Palermoite and goyazite, two strontium minerals from the Palermo Mine, North Groton, New Hampshire (abs.). *Am. Mineral.* **38,** 354.

ROSENZWEIG, A. AND J. J. FINNEY (1959) The unit cell of carminite. *Am. Mineral.* **44,** 663–665.

STRUNZ, H. (1960) Isotypie Palermoit-Carminit. *Neues Jahr. Mineral.* 1960, 49–62.

WEISZ, O., W. COCHRAN AND W. F. COLE (1948) The accurate determination of cell dimensions from single crystal x-ray photographs. *Acta Cryst.* **1,** 83–88.

WOOD, J. H. AND G. W. PRATT (1957), Wave functions and energy levels for Fe as found by the unrestricted Hartree-Fock method. *Phys. Rev.* **107,** 995–1001.

Manuscript received, July 19, 1962; accepted for publication, October 1, 1962.